LOOK ACADEMIC PUBLISHERS
OPEN ACCESS

INTERNATIONAL JOURNAL OF ENVIRONMENTAL & SCIENCE EDUCATION
e-ISSN: 1306-3065
2018, Vol. 13, No. 3, 265-274

Preparation and Evaluation of Optical Properties of $MnFe_2O_4/ZrO_2$ Nanocomposite

Mohammad Reza Jalali [1*], Hossein Salavati [2], Amir Ali Reza Goosheh [1], Azam Ahmadi Jeshvaghani [1]

[1] *Department of Physics, Payame Noor University, P.O.Box 19395-4697, Tehran, IRAN*
[2] *Department of Chemistry, Payame Noor University, P.O.Box 19395-4697, Tehran, Iran*

* CORRESPONDENCE: ✉ mrjalali93@yahoo.com

ABSTRACT

Degradation of organic pollutants such as synthetic dyes, which have a deleterious effect on the lives of humans, has extensively become the aim of researches in today's scientific world. Advanced oxidation processes (AOPs) such as photocatalysis has carried out, as useful methods for mineralizing organic pollutants in aqueous media via irradiating the nanocomposite by UV. In present work, $MnFe_2O_4/ZrO_2$nanocomposite was prepared via impregnation technique and characterized by using XRD, FT-IR and SEM. The photocatalytic activity of the supported $MnFe_2O_4$ was examined via degradation of different dyes (Methylene Blue and Methyl Orange,), then some parameters such as pH, the amount of photocatalyst, irradiation time, temperature and oxygen flow were optimized in order to improve the reaction yield of destruction of different dyes. The obtained results confirmed that the prepared composite had a great photocatalytic and sonocatalytic activity against different dyes in aqueous media.

Keywords: $MnFe_2O_4$, ZrO_2, impregnation, photocatalytic, nanocomposite, organic pollutants

INTRODUCTION

In today's life, environmental pollution has far-reaching negative consequences in the lives of humans. Heterogeneous photocatalytic destruction of organic pollutants in wastewater by using UV light as the excitation energy is an appealing field (Chen, 2000; Dressellhaus, 2002; Salavati & Kohestani, 2013; Sepelak, Heitjans, & Becker, 2007; Verma, 2004). To meet the need of this, it is important to design and prepare efficient photocatalytic materials, which may then appear to be a challenge to the chemists, at the same time, it also provides some opportunities for them. ZrO_2 is the most widely investigated heterogeneous semiconductor photocatalyst (Li, Chen, & Harris, 2018; Liu, Li, & Cui, 2007; Salavati et al., 2011, 2012; Zheng, 2018). Both of ZrO_2 and Spinel share the very similar photocatalytic processes owing to their similar electronic attribute. Although Spinel exhibit UV-light photocatalytic activity in homogenous system, the main disadvantages of them as photocatalysts lie in their low surface area and difficulty of separation from the reaction mixture. Therefore, development of novel solid catalysts with advanced characteristics such as surface area and porosity has been a challenge for a long time. In addition, for the purpose of practical application of this technique, immobilization of soluble spinel into some matrixes to prepare solid or supported spinel photocatalysts is essential. These insoluble $MnFe_2O_4/ZrO_2$ Nanocomposites exhibited much higher UV-photocatalytic activity than that of the corresponding pure or homogeneous spinel. Moreover, it is easy to separate and recover them for recycling purpose. In order to improve the photo efficiency of either $MnFe_2O_4$ or ZrO_2, and immobilization of soluble spinel, we here prepared nanocomposites $MnFe_2O_4/ZrO_2$via combining the methods of sol–gel and hydrothermal treatment. That is, $MnFe_2O_4$ has empty d orbits and can be used as

Article History: Received 10 February 2018 ◆ Revised 20 April 2018 ◆ Accepted 24 May 2018

Table 1. Structure of dyes used in this study

Dye	Chemical formula	MW (g/mol)	λ_{max}
Methylene Blue (MB)	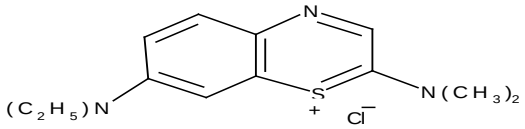	373.88	663
Methyl Orange (MO)	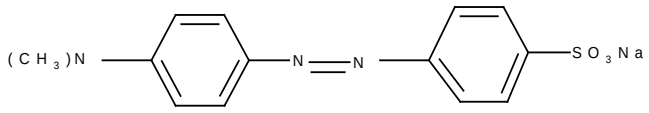	327.34	462

good electron acceptors. After the addition of spinel into ZrO_2 photocatalytic systems, the fast charge-pair (h^+ e^-) recombination on ZrO_2 can be retarded effectively. That is, Spinel has the ability to enhance the rate of conduction band (CB) electron transfer by accepting e^- (photogenerated electrons) to its empty d orbits. Recent studies have showed that reactive dyes can be decolorized by advanced oxidation process (Levec & Pintar, 2007) involving the generation of powerful oxidizing agent like hydroxyl radicals (OH^o), which destroy the pollutants in wastewater. The hydroxyl radicals are capable of mineralizing all organic compounds almost to carbon dioxide (CO_2) and water (H_2O) as well as other simple inorganic ions. Heterogeneous photocatalysis through illumination of UV (Sepelak, Baabe, Mienert, & Litterst, 2003) or solar light (Gateshki, Petkov, & Pardhan, 2005) on a semiconductor surface is an attractive advanced oxidation process. Here, we report the efficient UV light induced photocatalytic different dyes by in aqueous solutions.

RESEARCH METHODS

Synthesis of ZrO_2 Nanoparticles Hydrothermal Method

ZrO_2 nanoparticles were synthesized by hydrothermal method; as summarized by flow charts in **Figure 1**, In hydrothermal method, 0.01 mole zirconium nitrate hydrate (3g) was dissolved in 40cc double-distilled water and 30cc 1,4-butandiol as dispersing agent (Kirchberg, 2017). Then, the solution was stirred for 30 min at T = 40 ºC with pH = 5.8. Ammonia (25 wt %) was added drop by drop to the solution to achieve a final pH = 10 at room temperature. After formation of white slurry- like colloidal sol, it was further slowly heated at T = 80ºC for 10h in an open bath until a light-brown wet solid precipitation was obtained by evaporation of the solvents. In this hydrothermal process, essential chemical reactions take place between In^{3+} ions and ammonia (as mineralizer), for preparation of the ZrO_2 powders (Mahato& Banerjee, 2004). In the final stage, the wet precipitation was fully dried by direct heating on the hot plate at T = 150ºC for 8h. A white–grey powder was the final product.

Post-annealing of the ZrO_2 Nanocomposite

The precursor powders obtained by hydrothermal method were grounded in the glassy mortar to be turned into fine powders. Then, powders were heated in a Pyrex crucible to T = 450ºC and calcined for 8h, in an electric box furnace, and finally cooled down to room temperature. By post-annealing of the powders, all of the organic compounds were completely decomposed and ZrO_2 nanoparticles obtained (**Figure 1**).

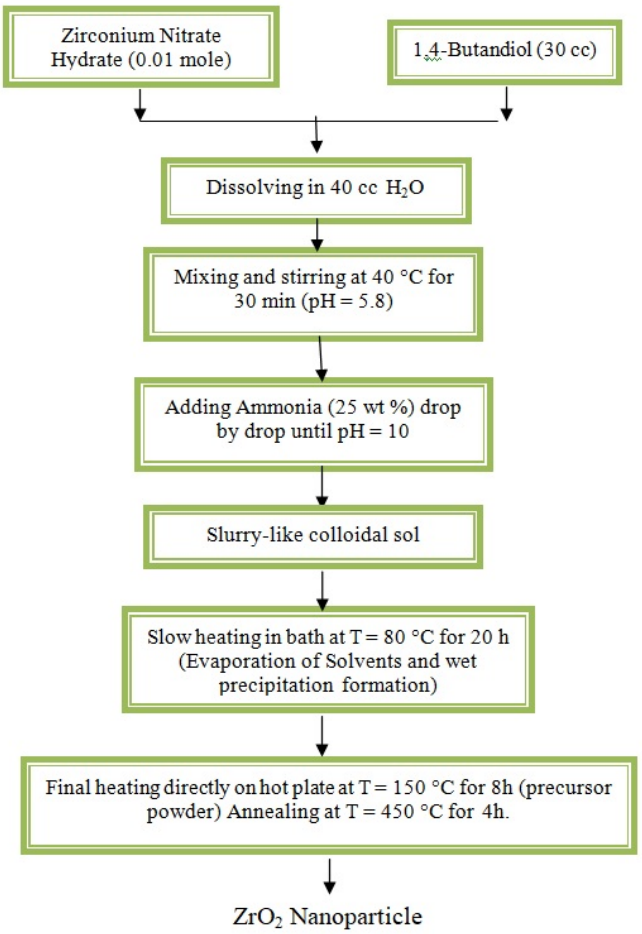

Figure 1. The flow chart for preparation of ZrO2 nanoparticles

Synthesis of $Mn_2Fe_2O_4/ZrO_2$ Nanocomposite by Sol-gel Method

A solution of ZrO_2 in ethanol (25 mL) was stirred at 80 °C, and then the mixture was slowly cooled to ambient temperature. Afterward, the acidity of the mixture was adjusted to pH=2 by using hydrochloric acid. To the resulting mixture was dropwise added $MnFe_2O_4$ (3.08 g) dissolved in the mixed solution of 25 mL ethanol and 10 mL of water, which was maintained under constant stirring for 3 h until gelling. After gelation, the solid was filtered and dried in air at 100 °C for 24 h. The dried gel was calcined in a vacuum at 350 °C for 4 h to fasten theZrO_2 network and washed with hot water (80 °C) three times (**Figure 2**).

General Procedure for Photocatalytic Degradation of Dyes

The catalytic activity of the nanocomposite was tested using Methyl Orange and Methylene Blue as the targets. A general photocatalytic method was carried out as following: 20 mg of $MnFe_2O_4/ZrO_2$nanocomposite was suspended in 10 mL of fresh aqueous dye solution (the dyes concentration is shown in **Table 2**). The lamp was inserted around the suspension after its intensity became stable. Photodegradation of dye was carried out in an open vessel using oxygen as oxidant. After the reaction finished, the suspensions were centrifuged and filtered, the photolyte was analyzed by UV–Vis.

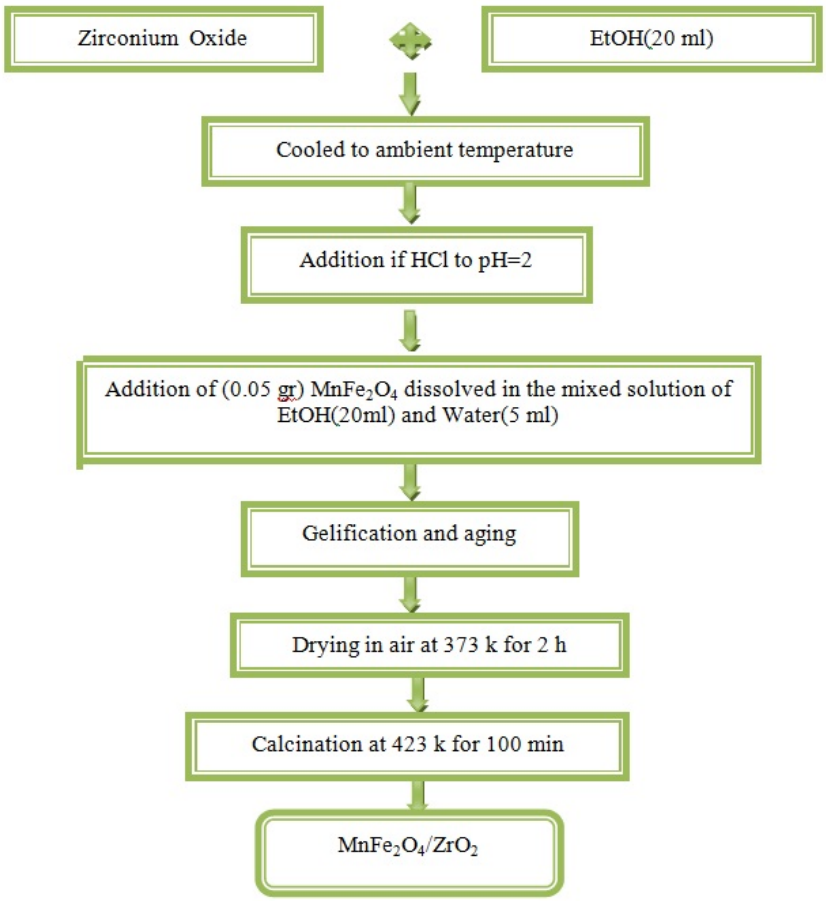

Figure 2. The flow chart for preparation of MnFe2O4/ZrO2 nanocomposite

Table 2. Photocatalytic, sonocatalytic and sonophotocatalytic degradation of dyes catalyzed by $MnFe_2O_4/ZrO_2$.[a]

Dye	ZrO_2 (Photocatalytic)			$Mn_2Fe_2O_4/ZrO_2$ (Photocatalytic)			$Mn_2Fe_2O_4/ZrO_2$ (Photocatalytic)			$Mn_2Fe_2O_4/ZrO_2$ (Photocatalytic)			$Mn_2Fe_2O_4$ (Photocatalytic)			Conc. (ppm)
	Yield (%)	Time (min)	k (min^{-1})	Yield (%)	Time (min)	k (min^{-1})	Yield (%)	Time (min)	k (min^{-1})	Yield (%)	Time (min)	k (min^{-1})	Yield (%)	Time (min)	k (min^{-1})	
Methylene Blue	21.5 ± 1.6	15	0.33	8.5 ± 1.2	15	0.14	90 ± 1.4	5	0.6	98 ± 1.3	5	0.92	48 ± 1.4	15	0.042	10
Methyl Orange	8.1 ± 1.3	15	0.005	26 ± 1.4	15	0.049	30 ± 1.4	5	0.17	78 ± 1.2	5	0.25	20 ± 1.5	15	0.011	20

[a] Reaction conditions: Catalyst (20 mg); Optimum pH; Oxygen flow rate=5 mL/min (N=4)

RESULT AND DISCUSSIONS

Catalyst Characterization

It is well-known that the catalytic activity of nanocomposites is strongly dependent on the shape, size and size distribution of the particles. Therefore, it is of paramount importance to characterize the microstructure of the nanocomposite. **Figure 3** shows the SEM images of the ZrO_2 nanoparticles and $MnFe_2O_4/ZrO_2$nanocomposite. SEM image reveals that powder is composed of aggregated extremely fine particles. From this image, it is evident that particles have a homogeneous shape. The particles sizes of the ZrO_2 and $MnFe_2O_4/ZrO_2$nanocomposite are prepared by a Sol-gel method.

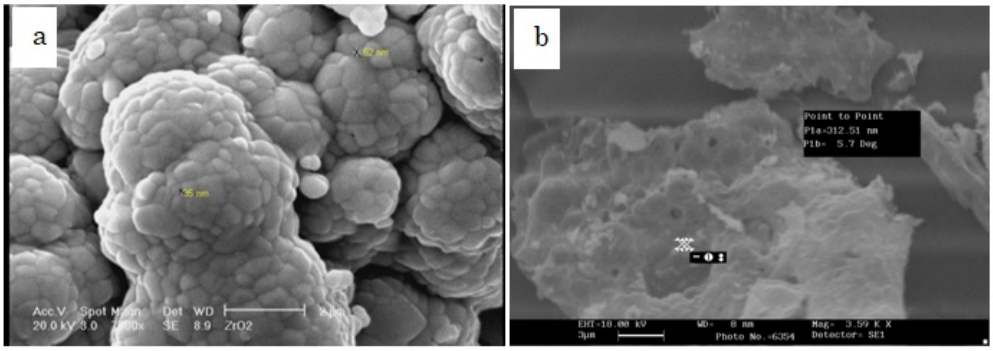

Figure 3. The SEM image of (a) ZrO2 nanoparticles ;(b) MnFe2O4/ZrO2

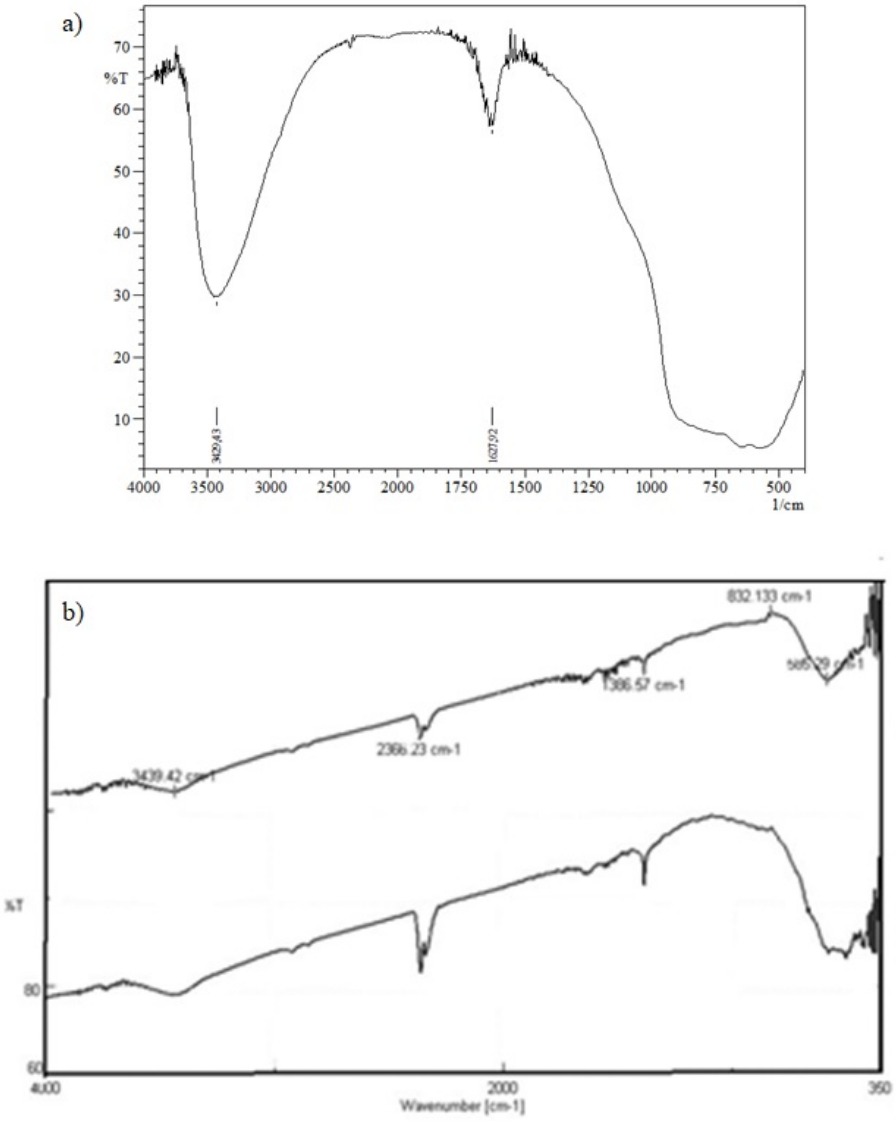

Figure 4. The FT-IR patterns of the MnFe2O4 ;(b) MnFe2O4/ZrO2 nanocomposite

Figure 4 shows the FT-IR spectrum of the $MnFe_2O_4/ZrO_2$nanocomposite, The IR characteristic bands of $MnFe_2O_4$ in the $MnFe_2O_4/ZrO_2$ nanocomposite have some red shifts compared with those for the pure $MnFe_2O_4$ (Mornet, Vasseir, Grasset, & Duguet, 2004; Candeia, Souza, & Bernard, 2006). Therefore, it is confirmed that a strong chemical interaction, not simple physical absorption, exists between the polyoxometalate and ZrO_2 surface.

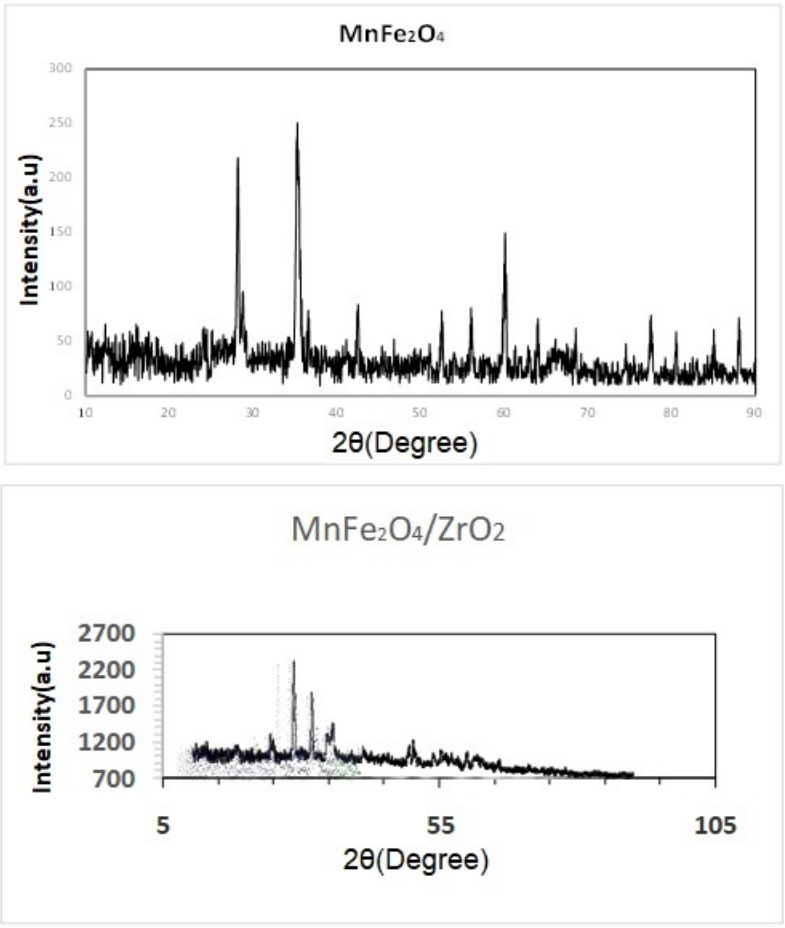

Figure 5. The XRD patterns of the MnFe2O4 ;(b) MnFe2O4/ZrO2 nanocomposite

The XRD patterns of $MnFe_2O_4$and$MnFe_2O_4/ZrO_2$ have been shown in **Figure 5** respectively. the characteristic diffraction Peaks at the XRD patterns of $MnFe_2O_4$ at (29.5), (34.5) & (38.5), are observed in the XRD patterns of $MnFe_2O_4/ZrO_2$ with lower intensity, changes in the peak positions and widths happened, It is clear that the changes are for immobilization of $MnFe_2O_4$ into matrix ZrO_2, The average particle size of $MnFe_2O_4/ZrO_2$ powder was calculated from XRD line broadening using the Debye–Scherer equation, $D= (0.89\lambda)/(\beta 1/2\cos\theta)$, where λ is the wavelength for Cu K_α radiation, β1/2 is the full width at half maximum (FWHM) and θ is the Bragg angle. The range of the particle size calculated is about 36 -86 nm.

Photocatalytic Degradation of Dyes

The results showed that the degradation percent was 85.0 % after irradiation of UV-Vis for 15 min at 25 ± 1 ºC. The effect of pH of solution was also investigated on the degradation rate of MB. The effect of pH on the degradation of dyes in the presence of $MnFe_2O_4/ZrO_2$ has been explained on the basis of point of zero charge (pH_{pzc}) of ZrO_2 particles. ZrO_2 is positively charged in acidic solution and negatively charged in alkaline solution. According to this explanation and because of electrostatic interactions, cationic dyes such as MB should be degraded at alkaline solution and anionic dyes such as methyl orange should be degraded effectively in acidic solutions.

Our results showed that positively and negatively charged dyes are degraded efficiently at acidic solutions. One explanation is that produced oxidizing agents such as H_2O_2 molecules are unstable in alkaline solution and therefore, the degradation of dyes decreases in alkaline solution. Despite of this explanation, photodegradation of MB in water by UV irradiated TiO_2 at pH= 3 have been reported (Fabiana, Lucía, Santos, & Cámara, 2001; Geetha& Ramesh, 2017; Sheats, 2004; Vautier, Guillard, & Herrmann, 2001). As Shimizu and coworkers have indicated, it is difficult to explain the main effect of pH (Pimachev, Kolesov, Chen, Wang, & Dahnovsky, 2012). These differences in the optimal pH for degradation rise from this fact that the point of

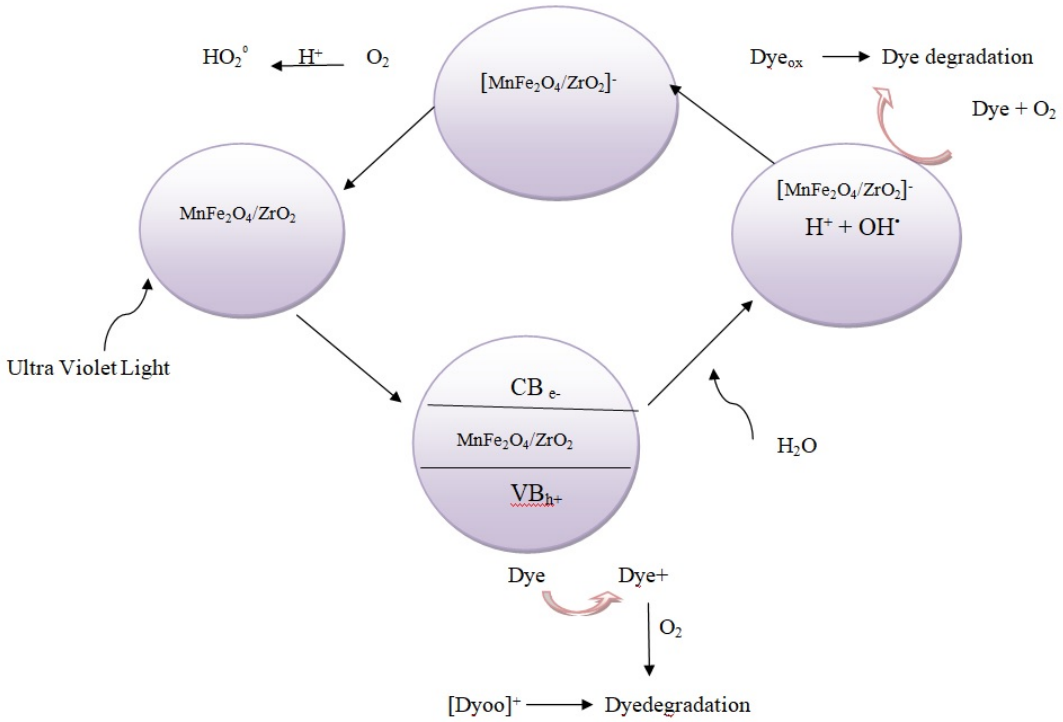

Figure 6. A plausible pathway for degradation of dyes

zero charge depends on the nature of dispersion, the difference of diameter and the type of catalyst. And finally, in the case of $MnFe_2O_4/ZrO_2$, the pH_{zpc} may be changed due to the presence of polyoxometalate and shows characteristics which if different from pure ZrO_2.

When the reaction was carried out in the absence of oxygen, the degradation percent was 62%. While, in a flow of 5 mL/min of oxygen gas, the highest degradation yield was obtained. Therefore, the presence of oxygen gas is necessary for dyes degradation and the degradation of all dyes was carried out in the presence of oxygen gas. But increase oxygen Pressure, has no effect on degradation yield.

As shown in **Table 2**, the $MnFe_2O_4/ZrO_2$ is an efficient photocatalyst for degradation of organic dye pollutants under irradiation of UV-Vis light. However, a plausible pathway for degradation of dyes is shown in **Figure 6** (Li, 2005; Petrier & Suslick, 2000; Yang et al., 2005). The difference in the absorption efficiency between ZrO_2 and $MnFe_2O_4/ZrO_2$ can be explained by mechanism of dyes degradation catalyzed by $MnFe_2O_4/ZrO_2$. According to this mechanism the reactants (dyes and dioxygen) reached the surface and entered into the pores of the composites through diffusion, and then they were adsorbed on the surface and in the pores by a hydrogen bonding interaction between functional groups of dyes and surface hydroxyl groups of ZrO_2 support, where they were accessible to the active sites (Mn– O–Fe) anchored within the pore cavities.

Sonocatalytic Degradation of Dyes

The effect of ultrasonic irradiation on the dyes degradation by $MnFe_2O_4/ZrO_2$ was also investigated. The increase irradiation power has no effect on the dye degradation. The presence of in a $MnFe_2O_4/ZrO_2$ ultrasonic system should result in the formation of OH^0 in the irradiated solutions. Increasing in the formation of OH^0 can be explained by well-known mechanism of hot spots and sonoluminescence as follows. First, cavitation can be increased due to the heterogeneous nucleation of bubbles, resulting in the induction of hotspots in the solution. Very high temperatures can breach in these hot spots and can cause the pyrolysis of H_2O molecules to form OH^0 (Ge & Qu, 2004; Harada, Hosoki, & Kudo, 2001; Okitsu et al., 2005).

Catalyst Reuse

After the reaction was finished, the suspension was centrifuged, and the $MnFe_2O_4/ZrO_2$ catalyst easily recovered by sedimentation, and the recovered catalyst was treated with water and successively. These are too strong coordination interactions between $MnFe_2O_4$ unit and the zirconia surface. More importantly, the

Table 3. The results of MnFe2O4/ZrO2 catalyst reuse and Mo leached in the degradatin of MB by photocatalytic [a]

Run	MnFe2O4/ZrO2 (Photocatalytic)		
	Yield (%)	Time (min)	Mo leachedb (%)
1	85±1.2	15	1.4
2	83±1.3	15	1
3	83±1.6	15	0.4
4	82±1.7	15	0.2

[a]Reaction conditions: Catalyst (20 mg); Optimum pH; Oxygen flow rate= 5 mL/ min, bDetermined by ICP(N=4)

interaction between $MnFe_2O_4$ unit and ZrO_2 support is chemical rather than physical. Therefore, the composites can be reused more than four times without finding obvious decreases of their photocatalytic activity (Wang et al., 2007). The results are summarized in **Table 3**.

CONCLUSION

This system introduces a simple and green heterogeneous photocatalytic approach for the degradation of organic pollutants. The prepared composite was successfully used for photocatalytic and sonocatalytic degradation of different dyes in aqueous media. The high catalytic activity of $MnFe_2O_4/ZrO_2$ is attributed to the synergistic effect between the $MnFe_2O_4$ and the ZrO_2. The $MnFe_2O_4/ZrO_2$ catalyst can be easily separated and recovered.

Disclosure statement

No potential conflict of interest was reported by the authors.

Notes on contributors

Mohammad Reza Jalali – Department of Physics, Payame Noor University, P.O.Box 19395-4697, Tehran, Iran.

Hossein Salavati – Department of Chemistry, Payame Noor University, P.O.Box 19395-4697, Tehran, Iran.

Amir Ali Reza Goosheh – Department of Physics, Payame Noor University, P.O.Box 19395-4697, Tehran, Iran.

Azam Ahmadi Jeshvaghani – Department of Physics, Payame Noor University, P.O.Box 19395-4697, Tehran, Iran.

REFERENCES

Candeia, R. A., Souza, M. A. F, & Bernard, M. I. B. (2006). $MgFe_2O_4$ pigment obtained at low temperature. *J. Mater. Res., 41*, 183-190. https://doi.org/10.1016/j.materresbull.2005.07.019

Chen, N. S., Yang, X. J., Liu, E. S., & Huang, J. L. (2000). Reducing gas-sensing properties of ferrite compounds MFe_2O_4(M=Cu, Zn, Cd and Mg). *J Sens Actuat. B., 66*, 178-180. https://doi.org/10.1016/S0925-4005(00)00368-3

Dressellhaus, M. S., Lin, Y. M, Rabin, A. J. O., Filho, A. G. S., Pimenta, M. A., Saito, R., Samsonidze, G. G., & Dresselhaus, G. (2002). Nanowires and nanotubes. *Mater. Sci, Eng. C., 1008*, 1-12.

Fabiana, Y. O., Lucía, A. B., Santos E, & Cámara, O. R. (2001). Photoelectrochemical characterization of nanocrystalline TiO_2 films on titanium substrates. J. Photochem. Photobiol. *A. Chem., 146*,175-188.

Gateshki, M., Petkov, V., & Pardhan, S.K. (2005). Structure of nanocrystalline $MgFe_2O_4$ fromX-ray diffraction, Rietveld and atomic pair distributionfunction analysis. *J. Appl. Cryst., 38*, 772-779. https://doi.org/10.1107/S0021889805024477

Ge, J., & Qu, J. (2004). Ultrasonic irradiation enhanced degradation of azo dye on MnO_2. *Appl Catal B: Environ., 47*, 133-140. https://doi.org/10.1016/j.apcatb.2003.08.001

Geetha, D., & Ramesh, P. S. (2017). Development of CuO doped Cts/PEG/Ag nanocomposite and their photodegradation efficiency of MB under natural Sunlight. *Materials Today: Proceedings, 4*, 4434-4444. https://doi.org/10.1016/j.matpr.2017.04.015

Harada, H., Hosoki, C., & Kudo, A. (2001). Overall water splitting by sonophotocatalytic reaction: the role of powdered photocatalyst and an attempt to decompose water using a visible-light sensitive photocatalyst. *J. Photochem. Photobiol. A: Chem. 141*, 219-224. https://doi.org/10.1016/S1010-6030(01)00445-2

Kirchberg, K., Becker, A., Bloesser A, Weller T, Timm J, Suchomski C, & Marschall R. (2017). Stabilization of Monodisperse, Phase-pure MgFe Nanoparticles in Aqueous and Non-aqueous Media and Their Photocatalytic Behavior. *J Phys Chem. C.*, 1-15.

Levec, J., & Pintar, A. (2007). Catalytic wet-air oxidation processes: A review. *Catal Today., 124*, 172-184. https://doi.org/10.1016/j.cattod.2007.03.035

Li, L., Wu, Q., Guo, Y., & Hu, C. (2005). Nanosize and bimodal porous polyoxotungstate–anatase TiO_2composites: Preparation and photocatalytic degradation of organophosphorus pesticide using visible-light excitation. *Micropor Mesopor Mater., 87*, 1-9. https://doi.org/10.1016/j.micromeso.2005.07.035

Li, Q., Chen, Y., & Harris, V. G. (2018). Particle-size distribution modified effective medium theory and validation by magneto-dielectric Co-Ti substituted BaMferrite composites. *J. Magn. Mater, 453*, 44-47. https://doi.org/10.1016/j.jmmm.2018.01.013

Liu, C. P., Li, M. W., & Cui, Z. (2007). Comparative study of magnesium ferrite nanocrystallites prepared by sol–gel and co precipitation methods. *J. Mater. Sci., 42*, 6133-6138. https://doi.org/10.1007/s10853-006-1070-z

Mahato, D. K., & Banerjee, S. (2017). Dielectric characteristics of $MgFe_2O_4$ ferrite prepared by sol-gel auto-combustion method. *Mat Today., 4*(4), 5525-5531. https://doi.org/10.1016/j.matpr.2017.06.008

Mornet, S., Vasseir, S., Grasset, F., & Duguet, E. (2004). Magnetic nanoparticle design for medical diagnosis and therapy. *J. Mater. Chem., 14*, 2161. https://doi.org/10.1039/b402025a

Okitsu, K., Iwasaki, K., Yobiko, Y., Bandow. H., Nishimura. R., & Maeda, Y. (2005). Sonochemical degradation of azo dyes in aqueous solution: a new heterogeneous kinetics model taking into account the local concentration OH radicals and azo dyes. *Ultrson. Sonochem., 12*, 255-262. https://doi.org/10.1016/j.ultsonch.2004.01.038

Petrier, C., & Suslick, K. (2000). Ultrasound-enhanced reactivity of calcium in the reduction of aromatic hydrocarbons. Ultrason. *Sonochem., 7*, 53-61. https://doi.org/10.1016/S1350-4177(99)00031-0

Pimachev, A., Kolesov, G., Chen, J., Wang, W., & Dahnovsky, Y. (2012). Internal relaxation in dye sensitized solar cells based on Zn_2SnO_4 nanostructures. *J. Chem. Phys., 137*, 244704-6. https://doi.org/10.1063/1.4772742

Salavati, H., & Kohestani, T. (2013) Preparation, characterization and photochemical degradation of dyes under UV light irradiation by inorganic–organic nanocomposite. *Mater Sci Semicond Process., 16*, 1904–1911. https://doi.org/10.1016/j.mssp.2013.07.014

Salavati, H., Tangestaninejad, S., Moghadam, M., Mirkhani, V., & Mohammadpoor-Baltork, I. (2011). Zirconia-supported Keggin phosphomolybdovanadate nanocomposite: A heterogeneous and reusable catalyst for alkene epoxidation under thermal and ultrasonic irradiation conditions. *C R Chimie., 14*, 588–596. https://doi.org/10.1016/j.crci.2011.03.003

Salavati, H., Tavakkoli, N., & Hosseinpoor, M. (2012). Preparation and characterization of polyphosphotungstate/ZrO_2 nanocomposite and their sonocatalytic and photocatalytic activity under UV light illumination. *Ultrason Sonochem., 19*, 546–553. https://doi.org/10.1016/j.ultsonch.2011.09.001

Sepelak, V, Heitjans, P., & Becker, K. D. (2007). Nanoscale spinel ferrites prepared by mechanochemical route. *J Therm Anal Calori., 90*, 93-97. https://doi.org/10.1007/s10973-007-8481-1

Sepelak, V., Baabe, D., Mienert, D., & Litterst, F. J. (2003). Magnetisation in nanocrystalline high-energy milled $MgFe_2O_4$. *J. Scr. Mater., 48*, 961-966. https://doi.org/10.1016/S1359-6462(02)00600-0

Sheats, J. R. (2004). Manufacturing and commercialization issues in organic electronics. *J Mat Res., 19*, 1974-1989. https://doi.org/10.1557/JMR.2004.0275

Vautier, M., Guillard, C., & Herrmann, J.-M. (2001). Photocatalytic Degradation of Dyes in Water: Case Study of Indigo and of Indigo Carmine. J. Catal., 201, 46-59. https://doi.org/10.1006/jcat.2001.3232

Verma, S., Joy P. A, Khollam, Y. B., Potdar, H. S., & Deshpande S. B. (2004). Synthesis of nanosized $MgFe_2O_4$ powders by microwave hydrothermal method. *J. Mater. Lett., 58*, 1092-1095. https://doi.org/10.1016/j.matlet.2003.08.025

Wang, J., Sun, W., Zhang, Z., Zhang, X., Li, R., Ma, T., Zhang, P., & Li, Y. (2007). Sonocatalytic degradation of methyl parathion in the presence of micron-sized and nano-sized rutile titanium dioxide catalysts and comparison of their sonocatalytic abilities. *J Mol Catal A: Chem., 272*, 84–90. https://doi.org/10.1016/j.molcata.2007.03.018

Yang, Y., Wu, Q., Guo, Y., Hu, C., & Wang, E. (2005). Efficient degradation of dye pollutants on nanoporous polyoxotungstate–anatasecomposite under visible-light irradiation. *J. Mol. Catal. A. 225*, 203-212. https://doi.org/10.1016/j.molcata.2004.08.031

Zheng, F., & Zhu, Z. (2018). Preparation of the $Au@TiO_2$ nanofibers by one-step electrospinning for the composite photoanode of dye-sensitized solar cells. *Materials Chemistry and Physics., 218*, 35-40. https://doi.org/10.1016/j.matchemphys.2018.01.021